IEEE Access
Multidisciplinary | Rapid Review | Open Access Journal

Received March 17, 2018, accepted May 3, 2018, date of publication May 14, 2018, date of current version June 29, 2018.

Digital Object Identifier 10.1109/ACCESS.2018.2836223

A 2D Ray-Tracing Based Model for Wave Propagation Through Forests at Micro- and Millimeter Wave Frequencies

NUNO R. LEONOR[1,2], (Member, IEEE), MANUEL GARCÍA SÁNCHEZ[3], (Member, IEEE), TELMO R. FERNANDES[1,2,4], (Member, IEEE), AND RAFAEL F. S. CALDEIRINHA[1,2,4], (Senior Member, IEEE)

[1]Instituto de Telecomunicações, 2411-901 Leiria, Portugal
[2]School of Technology and Management, Polytechnic Institute of Leiria, 2411-901 Leiria, Portugal
[3]Departamento de Teoría do Sinal e Comunicacións, University of Vigo, 36200 Vigo, Spain
[4]School of Engineering, University of South Wales, Pontypridd CF37 1DL, U.K.

Corresponding author: Rafael F. S. Caldeirinha (rafael.caldeirinha@ipleiria.pt)

This work was supported in part by the Portuguese Government through the Portuguese Foundation for Science and Technology, FCT, under Grant POPH/FSE, and in part by the Instituto de Telecomunicações, Portugal.

ABSTRACT This paper proposes the extension of a 2-D ray-tracing-based model for radiowave propagation in the presence of trees and vegetation areas to include real-sized trees and outdoor forest scenarios. The original propagation model proved to be suitable to characterize the electromagnetic behavior in the presence of indoor tree formation scenarios, despite some limitations found when applied to real-sized trees. In addition, the original propagation model requires the prior knowledge of the trees' re-radiation function to extract the relevant propagation input parameters, which is not always possible to obtain in outdoor scenarios. Therefore, an empirical method to extract the relevant input propagation parameters based on simple measurements is proposed. The performance of the proposed propagation model extension is extensively assessed in both the line-of-trees and tree formation scenarios, including various (and mixed) species, both in- and out-of-leaf foliation states, and at three signal frequencies. Finally, depending on the type of scenario, a benchmark between the proposed propagation model and both the radiative energy transfer (RET) and discrete RET (dRET) models, for line-of-trees and tree formation, respectively, is presented.

INDEX TERMS Millimeter wave radio propagation, modeling, ray tracing, scattering, vegetation.

I. INTRODUCTION

Recently, the millimeter-wave (mmWave) frequency band, ranging from 30 to 300 GHz [1], gained a lot of interest among the research community, since it will be the most likely solution to the next generation of radiowave communication systems.

In the last decades, several efforts have been made to characterize and model the electromagnetic behavior at such frequency bands. Nevertheless, the research community is yet far from fully understand the mmWave propagation phenomena in the presence of several types of obstacles. In the particular case of terrestrial mobile networks, wireless sensor networks, Infrastructure-to-Car and Car-to-Car communications in rural areas, the presence of trees and vegetation areas will substantially contribute to a degradation of the radio communication systems performance, causing signal attenuation (absorption), scattering and (de)polarization [2], [3]. Therefore, understanding the mmWave propagation phenomena in the presence of vegetation will be critical for next generation radio system design [4].

Empirical models derived from measurement results [5]–[12] have successfully been used to characterize the well-known "dual-slope" attenuation effect in various scenarios and frequency bands. Nevertheless, due to their site-specific nature, they usually lack of accuracy outside the model scope. On the other hand, theoretical models [13]–[19], [19], [21], [22] usually provide very reliable propagation phenomena predictions but, due to their mathematical complexity, and/or the extraction difficulty of the input parameters, e.g. leaf density, area and thickness, they tend to be cumbersome to apply in real-sized forests [23].

Ray-tracing based simulation platforms have been successfully used to predict the propagation phenomena in both indoor and outdoor urban scenarios. Nevertheless, in such simulation platforms, the phenomena inherent to the propagation through trees and vegetation areas are usually underestimated or neglected. In an effort to account for both coherent and incoherent (scattered) components usually found in vegetation media in ray-tracing based platforms, a propagation model has been proposed in [24] and [25], in which the canopy volume is assumed to consist of an ensemble of leaves and branches. The leaves are modeled as thin lossy dielectric disks and branches as finite lossy dielectric cylinders. This modeling approach was successfully used in [24] to predict the scattering phenomena of single and isolated trees, at 1.9 GHz, and latter extended to tree groups in [25]. Despite the relatively good prediction results depicted in [24] and [25], the input parameters required to properly apply the propagation model, include the number densities, size, and orientation statistics of branches and leaves, and the effective permittivity of branches and leaves, which may be prohibitively time-consuming to obtain in an inhomogeneous outdoor forest environments, preventing its applicability.

To this extent, a propagation model intended to predict the electromagnetic behavior in the presence of trees using a 2D ray-tracing based algorithm, has been presented in [26]. This model uses various point scatterers with specific re-radiation characteristics to describe the propagation phenomena in the presence of trees. This point scatterer formulation was successfully used, not only to predict the re-radiation pattern of single and isolated trees, but also the directional spectra inside various indoor tree formations, including mixed species, at 20 and 62.4 GHz. However, the proof-of-concept proposed in [26] was assessed on relatively small tree specimens and presented some limitations as far as its scalability to simulations in real forests was concerned. Namely in the input propagation parameter extraction method, since it requires the prior knowledge of the re-radiation function of all the trees present in the forest, which is not always easy or even possible to obtain in outdoor environments. Hence, an extension of a 2D ray-tracing based model for radiowave propagation in the presence of trees and vegetation areas to include real-sized trees and outdoor forest scenarios at millimeter wave frequency, is proposed. Additionally, the required input propagation parameter extraction method has been significantly simplified using empirical models, enabling the proper characterization of trees present in an outdoor forest scenario.

This paper is then organized as follows. Section II presents an overview of the propagation model originally proposed in [26], and its extension to include real-sized trees. The original propagation model requires the prior knowledge of the tree re-radiation pattern to extract the relevant input propagation parameters, which is not always easy or even possible to obtain in a real outdoor forest. Thus, an empirical method to extract the relevant input propagation parameters based on simple measurements is proposed in Section III. In Section IV, the propagation model is used to predict the electromagnetic behavior in outdoor line-of-trees scenarios. The propagation model is assessed not only, against measurements carried out in [27] in real forests, but also against the current ITU-R P833-8 recommendation [3] for propagation in vegetation. Section V presents the performance analysis of the propagation model while predicting the directional spectra inside an inhomogeneous outdoor tree formation with mixed species, at three frequencies. Similarly to line-of-trees scenarios, the directional spectra predictions are assessed not only against outdoor measurements, but a benchmark with dRET model is also provided. Finally, conclusions and directions for further work are drawn in Section VI.

II. 2D RAY-TRACING BASED MODEL FOR PROPAGATION THROUGH VEGETATION

A. ORIGINAL MODEL RATIONALE

The point scatterer formulation was successfully extended to indoor trees and vegetation areas in [26]. This propagation model makes use of various point scatterers with specific radiation characteristics to describe the electromagnetic behavior in the presence of indoor trees. Each tree is then characterized by a computational volume, which is composed by 10 point scatterers uniformly distributed in a circle with a radius that is 80% of the real tree radius, and with a set of input propagation parameters which includes:

- β, that regulates the forward lobe beamwidth of the scatterer function;
- Att_k, used to manage the amount of excess loss suffered by the propagation rays traveling through the tree volume.

The method proposed in [26] to extract the relevant propagation input parameters requires the prior knowledge of the re-radiation pattern of the specific tree to characterize, and relies on a two-step procedure. Firstly, the measured results are normalized to their maximum signal level, and several simulations are perform to evaluate the optimum β value, using the root-mean squared error (RMSE) criterion. Subsequently, in order to properly assess the appropriate insertion loss, both measured and simulated values are normalized to the free space (FS) signal level, and same RMSE criterion is used to extract the optimized Att_k parameter. A detailed description of this propagation model can be found in [26].

B. EXTENSION OF THE PROPAGATION MODEL TO REAL TREES

In [26], the 2D ray-tracing based model for propagation through vegetation was successfully used not only to predict the re-radiation pattern of 16 *Thuja plicata* and 13 *Ficus benjamina* trees, but also to predict the directional spectra inside various tree formations, including formations with some degree of inhomogeneity.

However, due to the reduced dimensions nature of indoor trees, some constraints of the propagation model were not observed in [26], since all measurements were performed in

the first slope of the dual-slope attenuation effect. In real forest scenarios, the second slope is easily observed due to the higher vegetation depths. For that purpose, two generic line-of-trees simulation scenarios have been deployed, and the 2D ray-tracing based model was used to predict the excess attenuation caused by the trees present in the radio path. In the scenario A, depicted in Fig. 1(a), the transmitter (TX) was placed at 4 m from a tree with 4 m of radius, and the receiver (RX) traveled along the tree diameter, from a vegetation depth of 0 to 8 meters. Since the aim of such simulations is to observe the attenuation phenomena, both TX and RX used directive antennas with 4° of half-power beamwidth (HPBW), to minimize the scattering components other than in the boresight of the antennas. In the simulation scenario depicted in Fig. 1(b), the tree was replaced by two smaller trees with 2 m of radius with same propagation characteristics, i.e. being characterized by the same set of input propagation parameters. To evaluate the excess loss of rays traveling through the vegetation volume, the propagation model proposed in [26] uses

$$L_{Ex} = 10\log_{10}(d \times Att_k + 1)\ [dB] \tag{1}$$

where, L_{Ex} is the excess loss given in decibel (dB), d is the distance traveled inside the vegetation volume given in meters and Att_k is a tree input parameter.

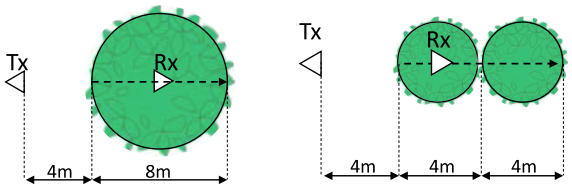

FIGURE 1. Real-size trees simulation example with a) 1 tree and b) 2 trees.

Since all trees used on these simulations have identical propagation characteristics, the predicted excess loss was expected to be similar in both scenarios. Nevertheless, due to the non-linearity of the attenuation model (1), by successfully applying the model for each tree, the attenuation is always evaluated using the first attenuation slope and the total excess loss is overestimated when two or more trees are to be considered.

Additionally, by successfully computing the excess loss given by (1) for various Att_k values, it was found that this attenuation model is severely limited regarding the gradient of the second attenuation slope. As one may observe in Fig. 2(a), different Att_k values will provide distinct first attenuation slopes. Nevertheless, a relatively narrow first attenuation slope is observed, i.e. under 2 m of vegetation depth, and second slope achieve stability very quickly (e.g. 3 dB of attenuation from 5 to 10 meters of vegetation depth). Furthermore, identical second slope gradients are found for different Att_k values. These facts revealed that for simulations with real-sized tree scenarios, a further enhancement to the attenuation model would thus be required.

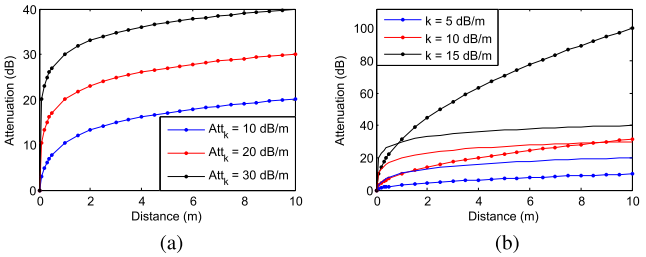

FIGURE 2. Attenuation given by the propagation model for various: a) Att_k and b) k values.

For that purpose, a survey was conducted on the empirical models present in the literature [5]–[10]. It was concluded that most of the empirical models characterize the attenuation caused by the presence of vegetation using

$$L_{Ex} = kd^n\ [dB] \tag{2}$$

where k and n are input parameters, usually optimized for a specific set of measurement results. Moreover, it was observed that the average value obtained for n parameter among the various empirical models, is around 0.5. Hence, for the purpose of this paper and to reduce the number of input parameters required to characterize a single tree, the n parameter was kept at 0.5.

Fig. 2(b) depicts the attenuation given by (2) for various values of k with $n = 0.5$. As one may observe, the propagation model (2) provides a larger control of the second attenuation slope and consequently, it seems to be more suitable to characterize the attenuation phenomenon in propagation through vegetation media.

Given these two limitations found for the original attenuation model, the extension of the 2D ray-tracing based propagation model to include real-sized trees and real outdoor scenarios has been developed as follows. Considering a generic scenario composed by N_T trees, as depicted in Fig. 3, the total excess loss $L_{Ex_{total}}$ of the rays traveling inside the vegetation volume, is given in dB, by

$$L_{Ex_{total}} = \sum_{i=1}^{N} k_i \left(d_i - d_{i-1}\right)^{0.5}\ [dB] \tag{3}$$

where, N_T is the number of the trees intersected, d_n is the total transmission distance, as depicted in Fig. 3, and k_i is an input parameter used to characterize the attenuation slope of the specific i^{th} tree.

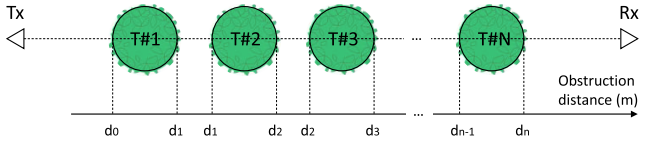

FIGURE 3. Generic simulation scenario.

Finally, the tree physical model originally defined in [26] is composed by 10 point scatterers uniformly distributed in a circle that is 80% of the real tree radius. This propagation

model was developed and optimized for relatively small indoor tree specimens. Hence, due to the increased number of scattering obstacles present in a real sized tree, such as leafs and branches, the number of point scatterers required to characterize the scattering behavior should also be increased. To this extent, in the 2D ray-tracing based model proposed herein, the number of point scatterers (N_{SCs}) used to characterize the tree physical model is given by

$$N_{SCs} = \lfloor 10T_R \rceil, \quad N_{SCs} \in \mathbb{N} \tag{4}$$

where T_R is the tree radius given in meters.

III. EMPIRICAL INPUT PROPAGATION PARAMETER EXTRACTION

A. INTRODUCTION

The propagation model [26] is proven to be suitable to predict both re-radiation phenomena of single and isolated trees and the directional spectra inside indoor tree formation scenarios. The enhancements proposed in previous section allow the propagation model to perform simulations in scenarios composed by real-sized trees. Nevertheless, the input propagation parameter extraction method defined in [26], relies on the prior knowledge of the re-radiation functions of all the trees present in the radio path, which is not always easy, or even possible, to obtain in a real forest scenarios.

In this section an empirical input parameter extraction method is proposed for both β and k parameters. Re-radiation measurements of 13 *Ficus benjamina* and 16 *Thuja pelicata* trees were conducted at two spot frequencies, 20 and 62.4 GHz. The tree specimens used to perform these measurements had roughly 60 cm of diameter and 1.5 m of height. More information about these tree specimens may be found in [18]. Subsequently, the relevant propagation input parameters were properly extracted according the method depicted in [26].

B. RE-RADIATION MEASUREMENTS AND INPUT PARAMETER EXTRACTION

The input parameter extraction method of the 2D ray-tracing based model for propagation through vegetation proposed in [26] requires the prior knowledge of the tree re-radiation pattern. Therefore, measurements intending to record the re-radiation pattern of 13 *Ficus benjamina* and 16 *Thuja pelicata* in-leaf trees, providing both sparse and dense leaf structures, respectively, were performed at 20 and 62.4 GHz. To minimize the antenna coupling contamination, particularly important in the side-scattering region, relatively narrow antennas were employed. The 20 GHz measurement system used 17° beamwidth 20 dBi standard horn antenna at both TX and RX ends, while the 62.4 GHz measurement system employed 9° beamwidth 25 dBi standard horn antennas.

The measurement geometry depicted in Fig. 4 was assembled in a controlled environment, inside an anechoic chamber, where the TX was placed at a distance of 1.15 m from the center of the tree under measurement (TUM), and the receiver (RX) was rotated along an arc around the tree, within

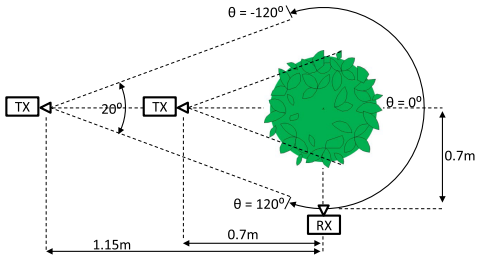

FIGURE 4. Tree re-radiation measurements geometry.

an angular range of $\theta = -120°$ to $\theta = 120°$, with increments of 1° at a constant distance of 0.7 m from the center of the tree. At each RX position, five measurement samples were acquired and the average signal level was calculated, thus minimizing any measurement system inaccuracies. Finally, the recorded signal levels were normalized with respect to the FS signal level acquired with the RX set at position $\theta = 0°$. Subsequently, all re-radiation measurements were repeated with the TX placed at a distance of 0.7 m from the center of the TUM. During these measurements, both TX and RX were set at a constant height of 1.4 meters above the ground.

The input propagation parameters β and k were extracted using the RMSE minimization process proposed in [26], for all the recorded re-radiation patterns. To this extent, the 2D propagation model was used in a re-radiation simulation geometry similar to that depicted in Fig. 4. Subsequently, in the first step, both measured and simulated results were normalized to their maximum signal level. Given that the tree insertion loss is managed by k parameter, by normalizing both signals to their maximum level, the influence of this parameter is substantially minimized, allowing proper fine tuning of β. Hence, several values of β were computed so that the ideal value was evaluated through a RMSE minimization process. Following β evaluation, both measured and simulated results were again normalized, but this time to the free space signal level. Such normalization will allow one to determine the appropriate insertion loss caused by the tree and, therefore, the proper evaluation of k parameter. This parameter is obtained using the same RMSE criteria. Tables 1 and 2 present a brief analysis of the optimized sets of propagation parameters obtained with the TX at a distance of 0.7 and 1.15 meters, respectively, along with the RMSE values obtained using

$$RMSE = \sqrt{\frac{\sum_{i=1}^{N}(Y_i - \hat{Y}_i)^2}{N}} \tag{5}$$

where Y_i and $\hat{Y}_i$ are the measurement results and model predictions in dB, respectively, and N is the number of measurement positions, i.e., receiver angles.

C. EMPIRICAL INPUT PARAMETER EXTRACTION METHOD

As aforementioned, the k parameter is used to manage the excess attenuation rate, in addition to free space loss, of the

TABLE 1. Extracted input parameters obtained at TX distance of 0.7 m.

		$\beta(^\circ)$		$k(dB/m)$		$RMSE(dB)$	
Species	Freq.	20	62.4	20	62.4	20	62.4
Ficus benjamina	Mean	23.6	23.3	14.2	13.9	6.7	7.1
	Max.	30.7	28.4	16.0	16.1	7.6	7.8
	Min.	17.7	14.7	12.4	11.8	5.8	6.3
	STD	3.9	4.5	1.2	1.2	0.7	0.5
Thuja pelicata	Mean	38.5	35.4	16.5	16.4	7.4	8.0
	Max.	50.0	50.0	17.8	17.4	9.1	11.6
	Min.	28.8	22.4	15.0	14.8	5.7	5.9
	STD	7.1	8.5	0.7	0.6	1.0	1.9

TABLE 2. Extracted input parameters obtained at TX distance of 1.15 m.

		$\beta(^\circ)$		$k(dB/m)$		$RMSE(dB)$	
Species	Freq.	20	62.4	20	62.4	20	62.4
Ficus benjamina	Mean	19.0	20.2	13.0	13.5	6.1	6.8
	Max.	33.1	31.3	14.9	16.1	6.8	7.4
	Min.	12.2	11.4	10.8	11.4	5.6	6.4
	STD	6.2	5.0	1.3	1.2	0.4	0.3
Thuja pelicata	Mean	36.5	34.9	15.8	16.1	6.6	7.5
	Max.	50.0	50.0	16.9	16.9	7.6	10.5
	Min.	22.3	20.4	14.6	15.0	5.7	6.3
	STD	6.5	8.5	0.5	0.6	0.6	1.2

rays traveling through the vegetation structure. In the particular case of the RX angle $\theta = 0^\circ$, this excess loss can be defined as tree insertion loss (I_L). Therefore, the optimized value of k obtained for a specific tree specimen, is expected to be strongly correlated with the measured I_L of that tree. The relation between the optimized values obtained for k and the respective measured tree insertion loss is depicted in Fig. 5. As one may observe, both k parameter and the I_L of the specific tree specimens are strongly correlated. Therefore, using a simple linear regression, the empirical model given by

$$k_{emp} = 8\left(\frac{I_L}{T_d}\right)^{0.2} \ [dB/m] \tag{6}$$

was obtained, where the empirical value of k (k_{emp}) can be extracted directly from the relationship between the measured I_L and the tree diameter (T_d).

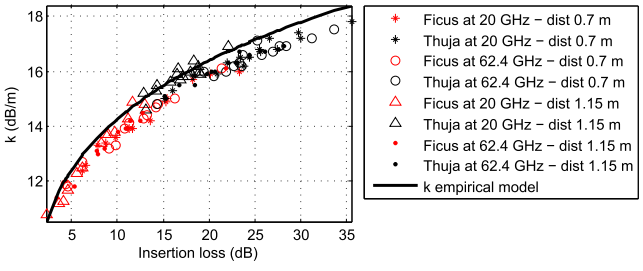

FIGURE 5. Optimized k parameter vs. tree insertion loss.

As far as β parameter is concerned, no direct relation between the input parameter and the available measurement data was found. Nevertheless, according to [28], the re-radiation function of a single and isolated tree can typically be represented by Gaussian shaped forward (main) lobe, superimposed to an isotropic level. Since β is used to manage the forward lobe beamwidth of the scatterer function, this parameter was analyzed against the measured front-to-side signal discrimination (G_{FS}), i.e. the relationship between the signal level recorded with the RX at position $\theta = 0^\circ$ and at position $\theta = 90^\circ$ (or $\theta = -90^\circ$), for all the re-radiation measurements. Fig. 6 depicts the optimized values obtained for β parameter and the respective measured G_{FS}.

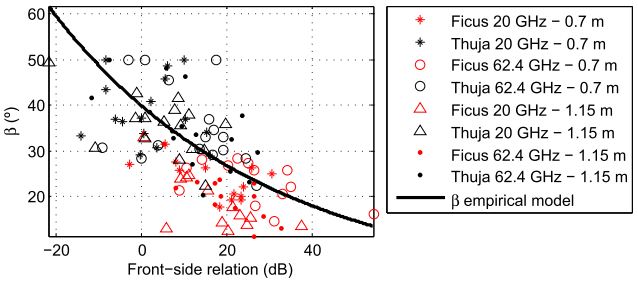

FIGURE 6. Optimized β parameter vs. front-side signal level discrimination.

As depicted in Fig. 6, the correlation between the optimized value obtained for β parameter and the respective measured G_{FS} is not as pronounced as the direct relation found for k parameter is. Notwithstanding, there is an evident trend line which can be described by

$$\beta_{emp} = 40e^{-0.02G_{FS}} \ [^\circ] \tag{7}$$

where the empirical β value (β_{emp}) can be extracted from 2 simple measurements, with the RX at position $\theta = 0^\circ$ and $\theta = 90^\circ$.

Despite the fact that using the empirical models (6) and (7) for input propagation parameter extraction will introduce errors in the single tree characterization, they severely simplify the extraction method proposed in [26], enabling the input parameter extraction in real outdoor forest scenarios, since only two simple measurements are required. That is, k is extracted directly from the measured tree insertion loss, and the β is derived from the front-to-side signal discrimination G_{FS}.

IV. PERFORMANCE ANALYSIS IN OUTDOOR TREE LINE SCENARIOS

A. INTRODUCTION

In this section, an assessment of the 2D ray-tracing based propagation model is performed using measurements in line-of-tree scenarios conducted under the research work presented in [27] in real forest scenarios, which was the basis to the current ITU-R P.833-8 recommendation for propagation in vegetation [3].

For validation purposes, the outdoor scenarios were carefully selected to include different tree species in both in- and out-of-leaf states, at various signal frequencies. Additionally, the performance of the proposed propagation model

is compared against the current ITU-R recommendation for propagation in vegetation [3].

B. METHODOLOGY AND MEASUREMENT GEOMETRY

Two different outdoor line-of-trees scenarios were selected for validation purposes. Regarding the measurement scenario #1, depicted in scale in Fig. 7(a), the transmitter was placed at a 10.8 m from the vegetation volume, composed by 12 London Plane (LP) trees. The normalized received signal was measured with the receiver placed at each one of the 13 measurement positions (MP), represented by the red dots. Measurements performed in scenario #1 were conducted at 11.2 GHz using a wideband channel sounder, which employed an 11 dBi X-band horn antenna with a half power beam width (HPBW) of 18° in both azimuth and elevation planes at the TX end, and an 11 dBi Angus horn antenna with a HPBW of 19.5° and 40.3° in azimuth and elevation planes, respectively, at the receiver end. These TX and RX antennas were set at a height of 3.5 meters from the ground level enabling the direct TX to RX path to travel through the middle of the canopy volume. Additionally, measurements in scenario #1 were conducted during two different seasons, providing both in- and out-of-leaf foliation states, scenario #1a and #1b, respectively. Detailed information about the measurement geometry and recorded signal levels is depicted in Table 3 for each one of the MP (MP1 to MP13), including the total propagation path given in meters, and the vegetation depth and the received signal levels, which are normalized with respect to the level recorded with the RX set at the first measurement point (MP1).

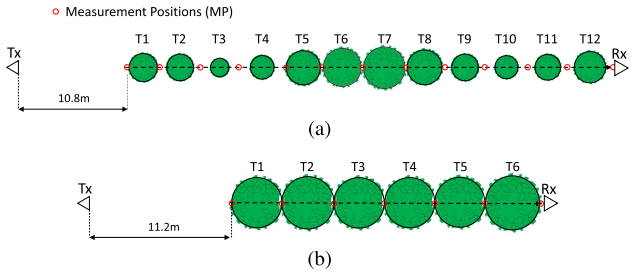

FIGURE 7. Measurement geometries in forests with real-sized trees: Scenario a) #1 and b) #2.

In the measurement scenario #2, represented in Fig. 7(b), similar geometry was selected using 6 in-leaf Silver Maple (SM) trees. Similarly to measurement scenario #1, the excess attenuation was recorded at each one of the 7 MP, MP1 to MP7, represented by the red dots, at two different signal frequencies, 36.5 and 61.5 GHz, #2a and #2b, respectively. In the 36.5 GHz measurement system, both TX and RX employed similar 24 dBi Lens horn antennas with a HPBW of 3.5° in both azimuth and elevation planes, while the 61.5 GHz measurement system used 34 dBi Lens horn antennas with a HPBW of 3° in both azimuth and elevation planes, for both TX and RX ends. Similarly to measurement scenario #1, both TX and RX heights were defined so that the electromagnetic signals traveling from TX towards RX intersected the middle of the canopy volume, found at a height of 3.2 meters from the ground level.

TABLE 3. Real forests measurement data.

	Total path (m)		Veg. depth (m)		Normalized Attenuation (dB)			
Pos.	#1	#2	#1	#2	#1a	#1b	#2a	#2b
MP1	10.8	11.2	0.0	0.0	0.0	0.0	0.0	0.0
MP2	14.0	15.1	2.7	3.9	6.4	6.9	12.4	15.3
MP3	18.0	19.1	5.3	7.9	16.7	32.1	25.4	29.3
MP4	21.8	23.1	7.1	11.9	24.0	24.2	32.2	34.6
MP5	26.3	27.0	9.4	15.8	20.8	26.3	40.6	36.6
MP6	29.8	30.9	12.8	19.7	31.9	30.1	39.8	54.7
MP7	34.0	35.2	16.5	24.0	33.2	34.6	41.8	62.0
MP8	38.0	-	20.6	-	37.1	44.9	-	-
MP9	42.0	-	24.0	-	32.7	37.6	-	-
MP10	45.9	-	26.5	-	47.7	37.2	-	-
MP11	50.1	-	28.7	-	33.9	34.4	-	-
MP12	54.0	-	31.2	-	36.3	41.1	-	-
MP13	58.4	-	34.3	-	38.5	42.2	-	-

As far as input propagation parameter extraction is concerned, the empirical method proposed in Section III could not be directly applied to these particular scenarios, since the I_L and G_{FS} parameters were not known for each one of the trees present in the radio path.

Nevertheless, the I_L parameter obtained for the first tree present in the vegetation structure can easily be derived from the first and second measurement points, MP1 and MP2, respectively, and since the tree diameter is known, the empirical model (6) can be applied. The same is not valid for the second tree, since the received signal in MP3 include both direct and diffuse scattering from the first tree. Therefore, and given that all the trees (in each scenario) are of the same species and foliation states, a rough approximation has been assumed and the k value extracted for the first tree, was used to characterize all the trees present in the simulation channel.

Given the measurement scenarios configuration, typically path-loss scenarios, the influence of β parameter is relatively reduced since measurements are not performed in side and back-scattering regions. Therefore, no great relevance was given to β parameter extraction, and the trees present in the simulation channels were characterized with the mean value found for β parameter in Section III, which is 29.4°.

C. ITU-R RECOMMENDATION

As aforementioned, a benchmark with current ITU-R recommendation [3] for propagation in vegetation is also provided. This propagation model is based on RET [16] theory, which treats the vegetation media as a random a homogeneous medium of scatterers with an infinitesimal size d_s. Each scatterer is characterized by a set of input parameters, including an absorption coefficient (σ_a), which describes the amount of the incoming radiation that is absorbed by the scatterer, the scattering cross section per unit of volume (σ_s), which

describes the amount of signal scattered by the medium element volume, and the directional scattering profile. The latter is normally expressed using the well-known phase function model, defined by

$$\rho(\gamma) = \alpha \left(\frac{2}{\beta}\right)^2 e^{-(\frac{\gamma}{\beta})^2} + (1-\alpha) \tag{8}$$

which represents a Gaussian function superimposed onto an isotropic background level, where α is the ratio between the forward lobe power and the total power of the phase function, β represents the half power beamwidth of the forward lobe and γ is the angular difference, in radians, between the incident and scattering directions. These input parameters are provided in [3] for various species, frequencies and foliation states.

TABLE 4. ITU-R model input parameters extracted from [3].

Scenario	Tree species	Foliated state	α	$\beta(^\circ)$	W	σ_τ (N_p/m)
#1a	LP	Out-of-leaf	0.95	19	0.95	0.459
#1b	LP	In-leaf	0.7	100	0.95	0.75
#2a	SM	In-leaf	0.85	53	0.875	0.444
#2b	SM	In-leaf	0.8	48	0.8	0.567

The input parameters extracted from [3] used to model the selected forest scenarios using RET theory, are depicted in Table 4 in terms of the extinction coefficient (σ_τ), which is given by $\sigma_\tau = \sigma_s + \sigma_a$, and the albedo ($W$), which is the ratio between the scattered power and the total power entering the random medium is expressed by

$$W = \frac{\sigma_s}{\sigma_s + \sigma_a}. \tag{9}$$

D. RESULTS AND ANALYSIS

The 2D ray-tracing based model for radiowave propagation through real forests scenarios was then used to predict the received signal level in all positions of the four simulation geometries previously described. The obtained results were assessed not only against the current ITU-R P833-8 [3], but also against outdoor measurements performed in line-of-trees scenarios.

Figs. 8(a) to (d) depict the results obtained for the selected forest scenarios. These results include the predictions of the proposed model in terms of total received signal level, the direct (coherent) component that travels from the TX to the RX through the vegetation volume, the RET predictions and measurement results. As one may observe, despite the fact that all relevant input propagation parameters could not be properly extracted for all trees present in the simulation channel, and the consequent rough assumption that all trees in each scenario have similar propagation characteristics, the proposed propagation model was able to provide very accurate signal level predictions since a relatively good agreement with measurement data was achieved.

Subsequently, a quantitative assessment on the performance of both modeling approaches, while predicting the

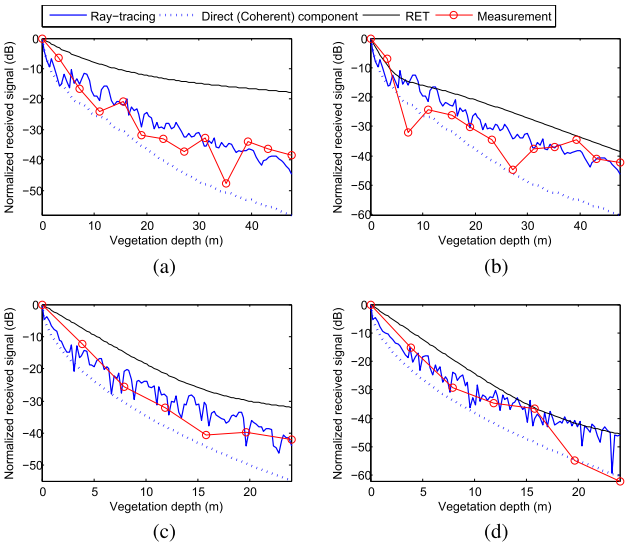

FIGURE 8. Results obtained in real forests: Scenario a) #1a, b) #1b, c) #2a and d) #2b.

propagation phenomena in real forests scenarios, was performed. For that purpose, the RMSE between the measured results and both the 2D ray-tracing based and the ITU-R models were obtained for each forest scenario, using equation (5). The RMSE values are depicted in Table 5. From these results one may conclude that the proposed propagation model, not only is able to provide a remarkably good performance, with an average RMS error of 6.2 dB, but also it outperforms the current ITU-R recommendation for propagation in vegetation in the four forest scenarios analyzed. Moreover, a better tree characterization and modeling of the individual real trees and/or the knowledge of their re-radiation pattern, would undoubtedly lead to significantly better results.

TABLE 5. RMS error obtained in real forest scenarios.

RMS errors (dB)					
Propagation model	Scenario				Mean
	#1a	#1b	#2a	#2b	
ITU-R P833.8	18.0	9.6	9.6	9.3	11.7
Proposed model	5.1	6.1	5.1	8.6	6.2

V. PERFORMANCE ANALYSIS IN REAL-SIZED TREE FORMATION SCENARIOS

A. INTRODUCTION

The 2D ray-tracing based model was proven to be suitable to characterize the propagation phenomena through outdoor line-of-trees scenarios, since a relatively good agreement between model predictions and measurement results was achieved.

In this section, the propagation model is used to predict the directional spectra inside an outdoor inhomogeneous tree formation. Measurements carried out in [18]–[20] at 11.2, 40

and 62.4 GHz, were used for validation purposes. Additionally, since the ITU-R recommendation uses RET theory, which is derived for infinitely extended homogeneous forests, a benchmark between the proposed model and the enhanced and discrete version of RET model, the dRET [17] model, is presented.

B. MEASUREMENT GEOMETRY AND INPUT PARAMETER EXTRACTION

The selected test forest, located in the North-West of Cardiff at the Glamorgan Wyevale Garden Center, is formed by 26 full size in leaf trees, labeled from T1 to T27, of six different species inhomogeneously distributed along an area of about 4000 m^2, as depicted in Fig. 9. The characteristics of each tree, e.g. the scientific name, the approximate canopy diameters and heights, as well as the corresponding label in Fig. 9, are depicted in Table 6. The received signal was measured with both the TX and the RX at a height of 6.5 meters from the ground level, and with the receiver placed at each one of the 10 positions, labeled from MP1 to MP10, where the receiving antenna was rotated around its vertical axis, from $\theta_{RX} = 0°$ to $\theta_{RX} = 360°$ according to the referential depicted in Fig. 9, with increments of 1°, recording the directional spectra in that particular position.

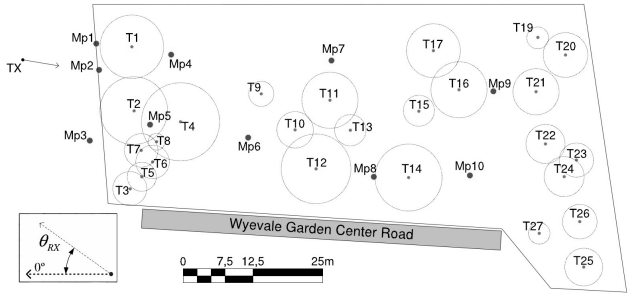

FIGURE 9. Scaled diagram of Wyevale Garden Center test site.

To enable a proper extraction of the relevant propagation input parameters required by the proposed model, additional measurements were performed intending to record the tree insertion loss and the front-to-side signal discrimination. These measurements were carried out using the measurement geometry depicted in Fig. 10. In the Wyevale test forest it was not possible to find isolated trees therefore, to confine the amount of interference from the remaining vegetation, and thus the propagation parameters were only extracted from the trees located in the border of the forest, i.e., $T_1, T_{11}, T_{12}, T_{17}$ and the ensemble of tree $T_{3;5;6;7}$. The normalized received signal levels recorded during these measurements are shown in Table 7, where $M_{1,3}$ is the difference between the maximum measured signals at M_1 and M_3, while $M_{1,2}$ stands for the difference between the maximum signal at M_1 and an average of the M_2 signal obtained for the $\pm 15°$ angular range around the center on the tree. The analysis of the results from Table 7 demonstrates that the sparser (T_1) and smaller ($T_{3;5;6;7}$) trees, tend to exhibit

TABLE 6. Tree species of Wyevale Garden Center site.

Tree Label	Scientific Name	Canopy Diameter (m)	Tree Height (m)
T_1	White Oak	11.4	10.9
T_2	Oleaster	12.1	16.5
T_3	Prunnus Sargentii	6.1	3.5
T_4	Oleaster	14.0	17.7
T_5	Prunnus Sargentii	5.2	3.5
T_6	Prunnus Sargentii	6.0	3.5
T_7	Prunnus Sargentii	6.0	3.5
T_8	Prunnus Sargentii	3.0	3.0
T_9	Betula Pendula	4.5	8.4
T_{10}	Betula Pendula	6.5	6.4
T_{11}	Betula Pendula	10.0	10.0
T_{12}	Oleaster	12.5	15.6
T_{13}	Betula Pendula	5.6	5.5
T_{14}	Oleaster	12.0	15.0
T_{15}	White Oak	5.6	2.5
T_{16}	White Oak	10.1	7.2
T_{17}	Prunus Avium	9.6	7.3
T_{19}	Pecan	3.9	8.9
T_{20}	White Oak	8.0	9.6
T_{21}	Pecan	8.3	5.2
T_{22}	Pecan	7.0	7.0
T_{23}	White Oak	6.1	7.8
T_{24}	White Oak	7.2	6.8
T_{25}	Pecan	6.8	13.0
T_{26}	Pecan	6.2	14.3
T_{27}	Pecan	3.9	4.3

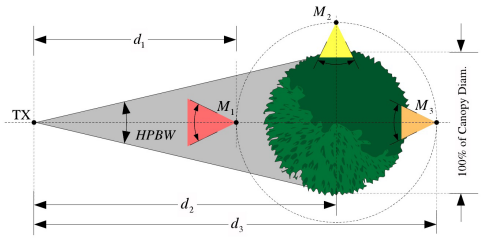

FIGURE 10. Measurement geometry for input parameter extraction.

higher signal levels at M_3 when compared with M_2. This suggests that the received signal at M_3 is still due to the coherent component, whereas the signal at M_2 is due to the scattered or diffused component. The remaining trees, exhibit similar signal levels at M_2 and M_3. Such similar levels, clearly indicates that the coherent signal component is completely attenuated inside the canopy volume and the signal received at M_3 was exclusively due to the incoherent (scattered) component, which is known to have an isotropic level around the tree. Additionally, the anticipated tendency for $M_{1,3}$ values to increase as the measurement signal frequency increases, is not always evident for all the trees under analysis, and opposite trend was often observed in Table 7. This phenomenon might be related with the fact that a greater Fresnel clearance will exists at higher frequencies, allowing

TABLE 7. Normalized mean received signal levels at M2 and M3 during the parameter extraction measurements.

Normalized mean levels (dB)						
Tree	11.2 GHz		40 GHz		62.4 GHz	
label	$M_{1,3}$	$M_{1,2}$	$M_{1,3}$	$M_{1,2}$	$M_{1,3}$	$M_{1,2}$
T_1	-29.9	-49.4	-27.8	-49.6	-25.4	-47.3
$T_{3;5;6;7}$	-38.0	-57.4	-29.5	-52.6	-49.9	-58.8
T_{11}	-45.4	-47.0	-37.7	-45.4	-43.7	-46.7
T_{12}	-48.1	-46.7	-37.7	-48.8	-41.2	-56.0
T_{17}	-44.3	-44.5	-26.7	-40.2	-37.9	-49.9

the radiowave signals, not only to penetrate the gaps in the foliage structure [2], but also to travel around the tree canopy, resulting in a stronger diffracted component, which may become predominant when compared with the total scattered component.

C. PROPOSED PROPAGATION MODEL SIMULATION GEOMETRIES

Given the flexibility of the proposed 2D ray-tracing based propagation model defining simulation scenarios, the geometry adopted to assess the model performance while predicting the directional spectra inside a tree forest is similar to that depicted in Fig. 9, where the transmitter was defined at about 10 m from the vegetation structure, composed by 22 trees, inhomogeneously distributed along the simulation channel. Trees labeled as T_3, T_5, T_6 and T_7 in Fig. 9, were modeled as a larger tree with same propagation characteristics.

According to (7), the empirical value of β can be extracted from G_{FS} therefore, using the measurement results depicted in Table 7, G_{FS} can be easily obtained using

$$G_{FS} = M_{13} - M_{12} \tag{10}$$

for the trees which M_{13} and M_{12} are known. Due to the lack of available measurements of the remaining tree specimens, same β values were used for different trees of same species.

As far as k parameter is concerned, M_{13} measurements were used to employ the empirical model (6). Since the measurement points M_1 and M_3 are not in the same place, the free space loss between M_1 and M_3 was evaluated to properly assess the I_L value of that specific tree. Hence, trees present in the simulation channel were characterized with a k derived from

$$k = 8\left(\frac{|M_{13}| - FSL_{13}}{T_d}\right)^{0.2} \quad [dB/m] \tag{11}$$

where FSL_{13} is the estimated FS loss between points 1 and 3, according to Friis equation, and T_d is the tree diameter. Table 8 depicts the relevant input propagation parameters used during these simulations, where $T_{3;5;6;7}$ is the ensemble of trees composed by T_3, T_5, T_6 and T_7.

TABLE 8. Proposed propagation model input parameters.

Tree	N_{SCs}	Frequency [GHz]					
		11.2	40	62.4	11.2	40	62.4
		$k[dB/m]$			$\beta[^\circ]$		
T_1	58	9.0	8.8	8.6	27.1	25.9	25.8
T_2	61	10.1	9.4	9.7	41.1	32.0	29.8
$T_{3;5;6;7}$	50	10.0	9.4	10.7	27.1	25.2	33.5
T_4	70	9.8	9.2	9.4	41.1	32.0	29.8
T_9	23	11.9	11.3	11.8	38.7	34.3	37.7
T_{10}	33	11.1	10.5	11.0	38.7	34.3	37.7
T_{12}	63	10.0	9.4	9.6	41.1	32.0	29.8
T_{11}	50	10.2	9.7	10.1	38.7	34.3	37.7
T_{13}	28	11.4	10.8	11.3	38.7	34.3	37.7
T_{14}	60	10.1	9.4	9.7	41.1	32.0	29.8
T_{15}	28	10.4	10.2	9.9	27.1	25.9	25.8
T_{16}	51	9.2	9.0	8.8	27.1	25.9	25.8
T_{17}	48	10.3	8.9	9.9	39.8	30.5	31.5
T_{19}	20	11.2	10.9	10.6	27.1	25.9	25.8
T_{20}	40	9.7	9.5	9.2	27.1	25.9	25.8
T_{21}	42	9.6	9.4	9.1	27.1	25.9	25.8
T_{22}	35	9.9	9.7	9.5	27.1	25.9	25.8
T_{23}	31	10.2	10.0	9.7	27.1	25.9	25.8
T_{24}	36	9.9	9.7	9.4	27.1	25.9	25.8
T_{25}	34	10.9	10.2	10.8	34.2	29.4	31.4
T_{26}	31	11.1	10.4	11.0	34.2	29.4	31.4
T_{27}	20	12.2	11.4	12.1	34.2	29.4	31.4

D. DRET SIMULATION GEOMETRY

As aforementioned, the ITU-R recommendation for propagation through vegetation [3] treats the vegetation media as a homogeneous media, and given the inhomogeneous tree distribution and the free space gaps between trees found in the selected test forest, the applicability of this modeling approach is limited. Encouraged by this limitation, a discrete version of the RET model was developed in [17]: the dRET model. The dRET model consists in dividing the vegetation structure into several non-overlapping cubic cells of identical dimensions. This discretization enables the RET theory to be applied on a vegetation volume with a certain degree of inhomogeneity and to be numerically solved for the unknown scattered intensities of the different vegetation cells. This is clearly an advantage over the original RET model, that is formulated for infinitely extended homogeneous forests. To this extent, the test forest depicted in Fig. 9 was divided in a 18×38 cell structure characterizing the inhomogeneous test forest, as illustrated in Fig. 11, where the filled cells represent the vegetation cells and the white cells represent the FS gaps between trees.

As far as vegetation cells are concerned, both RET and dRET use similar input propagation parameters with same physical and mathematical meanings. However, to distinguish both modeling approaches, a different notation was employed. To this extent, dRET vegetation cells are characterized by the absorption coefficient (k_a), the scatter cross section (k_s), the extinction coefficient (k_e), which is given

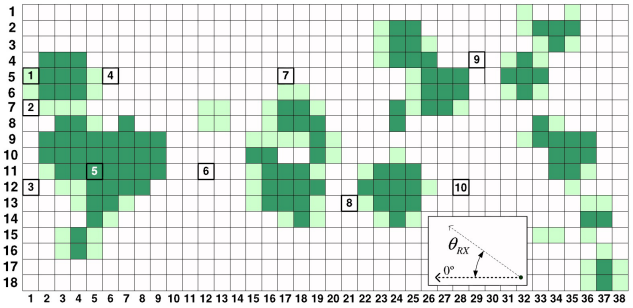

FIGURE 11. dRET model simulation geometry.

by $k_e = k_a + k_s$, and the phase function model presented in equation (8). The extraction method of the referred propagation input parameters are thoroughly detailed in [18]–[20], and subsequently, for the purpose of this paper, the dRET vegetation cells used to model the selected test forest were characterized according the set of input parameters provided in the latter.

E. MEASUREMENT RESULTS AND ANALYSIS

The 2D ray-tracing based propagation model was used to predict the directional spectra at each one of the 10 receiver positions, at 11.2, 40 and 62.4 GHz. Simulation results were assessed not only against dRET model predictions but also against measurements performed in an outdoor inhomogeneous test forest, comprised by 26 trees of 6 different species.

Results obtained at position MP3 at 62.4 GHz are depicted in Fig. 12(a). Since this measurement position is in line-of-sight (LOS), the received signal is mainly influenced by the receiver antenna radiation pattern. Nevertheless, scattered contribution can be found in the 100° to 260° angular range, where the proposed propagation model slightly overestimates the received signal level, yielding to a lower accuracy than that achieved by the dRET model.

At larger vegetation depths, the received signal is mainly influenced by the diffuse component caused by multiple scattering occurring within the vegetation structure, therefore it is harder to estimate the received signal accurately. Notwithstanding, a relatively good agreement between both the proposed propagation model and measurement results was achieved, when the receiver is placed at measurement positions, MP4, MP5, MP6, MP9 and MP10, depicted in Fig. 12(b) to (f), respectively. At larger vegetation depths and particularly at higher radiowave frequencies, the attenuation caused by the vegetation volume is increased. Hence, at some measurement positions and specific angular ranges, the received signal level was too low for the available dynamic range of the measurement system. To this extent, at some positions, measurements were performed in a limited angular range and the measurement in position MP10 could not be performed at 62.4 GHz.

A quantitative assessment on the performance of both modeling approaches, dRET and the proposed model, while

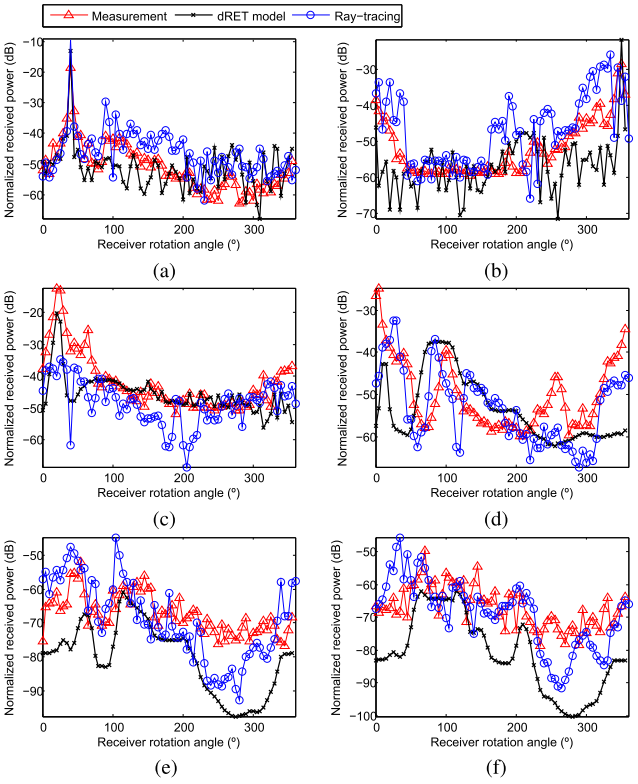

FIGURE 12. Directional spectra results obtained at position: a) MP3 and b) MP4 at 62.4 GHz; c) MP5 and d) MP6 at 40 GHz; and e) MP8 and f) MP10 at 11.2 GHz.

TABLE 9. RMS error obtained at 11.2, 40 and 62.4 GHz.

RMS error (dB)						
	Ray-tracing			dRET		
	Frequency [GHz]			Frequency [GHz]		
Pos.	11.2	40	62.4	11.2	40	62.4
MP1	7.6	10.1	9.7	4.9	8.0	7.9
MP2	8.7	8.7	9.4	3.7	8.4	8.3
MP3	8.9	6.2	7.3	7.5	8.0	7.5
MP4	8.5	5.4	8.5	11.6	9.4	8.6
MP5	7.4	9.6	11.2	9.2	7.6	17.6
MP6	10.3	8.6	10.6	13.8	11.7	16.1
MP7	9.4	5.3	5.8	6.6	7.4	11.3
MP8	9.8	7.3	11.4	15.2	17.8	21.6
MP9	9.5	11.7	10.3	6.8	6.5	7.9
MP10	9.3	7.1	N/A	16.3	7.3	N/A
Mean	8.9	8.0	9.4	9.6	9.2	11.9

predicting the directional spectra inside a tree formation was performed for all the available measurement data. To this extent, the RMSE between the measured results and both propagation models were obtained for each of the 10 positions, at 11.2, 40 and 62.4 GHz, using (5). Such performance indicators are depicted in Table 9. As already observed in MP3 at 62.4 GHz in Fig. 12(a), dRET model can provide slightly more reliable results at some positions. Nevertheless, a remarkably good performance was achieved by

the proposed propagation model, with a RMSE consistently below 12 dB, given its simplicity and ease of integration with other planning tools.

VI. CONCLUSIONS

In this paper, an extension of a 2D ray-tracing based model for radiowave propagation in the presence of trees and vegetation areas to include real-sized trees and outdoor forest scenarios, was successfully presented. Despite the fact that the enhancements included in the original propagation model are formulated for outdoor simulation scenarios, the final propagation model is also proven to be compatible with indoor tree specimens, providing an average RMSE error of 7 dB in re-radiation predictions of 13 *Ficus benjamina* and 16 *Thuja pelicata* trees, in two distinct re-radiation scenarios, at 20 and 62.4 GHz.

Additionally, the new propagation model was used to predict the signal attenuation in outdoor line-of-trees scenarios, including both in- and out-of-leaf foliation states, two different tree species, at three spot frequencies. When compared with measurements performed in a real forest scenario, the propagation model proved to provide reliable signal predictions, outperforming the current ITU-R P833-8.

Finally, the 2D ray-tracing based propagation model was used to predict the directional spectra inside an outdoor inhomogeneous tree formation at 11.2, 40 and 62.4 GHz. The performance achieved by this model was evaluated and assessed not only, against measurements, but also against the dRET model. Despite the fact that dRET model was able to provide more accurate predictions in some of the measurement points, the overall performance of the proposed propagation model was slightly better than that achieved by the dRET model, with an average RMSE below 9 dB.

Further work will be needed in an effort of extending the point scatterer formulation into a 3D ray-tracing based propagation model, to include trunk and ground layer effects and the interaction between layers. Additionally, time-varying input parameters should be analyzed to include dynamic effects, such as wind-induced dynamics or transmitter and/or receiver mobility.

REFERENCES

[1] F. Boccardi, R. W. Heath, A. Lozano, T. L. Marzetta, and P. Popovski, "Five disruptive technology directions for 5G," *IEEE Commun. Mag.*, vol. 52, no. 2, pp. 74–80, Feb. 2014.

[2] R. F. S. Caldeirinha, "Radio characterisation of single trees at micro- and millimetre wave frequencies," Ph.D. thesis, School Electron., Univ. Glamorgan, Wales, U.K., Apr. 2001.

[3] *Attenuation in Vegetation, Radiocommunication Assembly*, document ITU-R P.833-8, ITU-R, 2013.

[4] T. Rappaport and D. Sijia, "73 GHz wideband millimeter-wave foliage and ground reflection measurements and models," in *Proc. IEEE Int. Conf. Commun. Workshop (ICCW)*, London, U.K., Jun. 2015, pp. 1238–1243.

[5] M. Weissberger, "An initial critical summary of models for predicting the attenuation of radio waves by trees," Dept. Defense, Electromagn. Compatibility Anal. Center, Annapolis, MD, USA, Tech. Rep. ESD-TR-81-101, 1982.

[6] *Influence of Terrain Irregularities and Vegetation on Tropospheric Propagation*, document ITU-R CCIR 235-236, CCIR, 1986.

[7] M. Al-Nuaimi and R. Stephens, "Measurements and prediction model optimisation for signal attenuation in vegetation media at centimetre wave frequencies," *IEE Proc. Microw. Antennas Propag.*, vol. 145, pp. 201–206, Jun. 1998.

[8] M. O. Al-Nuaimi and A. M. Hammoudeh, "Measurements and predictions of attenuation and scatter of microwave signals by trees," *IEE Proc. Microw. Antennas Propag.*, vol. 141, pp. 70–76, Apr. 1994.

[9] COST 235, "Radio propagation effects on next-generation fixed-service terrestrial telecommunications systems—Final report," Luxembourg, 1995.

[10] Y. Meng, Y. Lee, and B. Ng, "Empirical near ground path loss modeling in a forest at VHF and UHF bands," *IEEE Trans. Antennas Propag.*, vol. 57, no. 5, pp. 1461–1468, May 2009.

[11] A. Seville and K. Craig, "Semi-empirical model for millimeter wave vegetation attenuation rates," *Electron. Lett.*, vol. 31, no. 17, pp. 1507–1508, Aug. 1995.

[12] A. Seville, "Vegetation attenuation modeling and measurements at millimetric frequencies," in *Proc. 10th Int. Conf. Antennas Propag.*, Edinburgh, Scotland, vol. 2, Apr. 1997, pp. 5–8.

[13] S. A. Torrico, H. L. Bertoni, and R. H. Lang, "Modeling tree effects on path loss in a residential environment," *IEEE Trans. Antennas Propag.*, vol. 46, no. 6, pp. 872–880, Jun. 1998.

[14] S. Torrico and H. Lang, "Wave attenuation prediction through a volume of random located lossy-dielectric branches—3-D vector transport theory," in *Proc. 6th Eur. Conf. Antennas Propag. (EUCAP)*, Prague, Czech Republic, Mar. 2012, pp. 3342–3345.

[15] K. L. Chee, S. A. Torrico, T. Kürner, "Radiowave propagation prediction in vegetated residential environments," *IEEE Trans. Veh. Technol.*, vol. 62, no. 2, pp. 486–499, Feb. 2013.

[16] R. Johnson and F. Schwering, "A transport theory of millimeter wave propagation in woods and forest," U.S. Army Commun.-Electron. Command, Forth Monmouth, NJ, USA, Tech. Rep. CECOM-TR-85-1, 1985.

[17] D. Didascalou, M. Younis, and W. Wiesbeck, "Millimeter-wave scattering and penetration in isolated vegetation structures," *IEEE Trans. Geosci. Remote Sens.*, vol. 38, no. 5, pp. 2106–2113, Sep. 2000.

[18] T. Fernandes, "A discrete RET model for millimeter-wave propagation in isolated tree formations," Ph.D. thesis, School Electron., Univ. Glamorgan, Wales, U.K., 2007.

[19] T. Fernandes, R. F. S. Caldeirinha, M. O. Al-Nuaimi, and J. Richter, "Radiative energy transfer based model for radiowave propagation in inhomogeneous forests," in *Proc. 64th IEEE Veh. Technol. Conf. (VTC Fall)*, vol. 1. Montreal, QC, Canada, Sep. 2006, pp. 1–5.

[20] T. Fernandes, R. F. S. Caldeirinha, M. O. Al-Nuaimi, and J. Richter, "Modelling radio wave propagation through vegetation media: A comparison between RET and dRET models," in *Proc. 2nd Eur. Conf. Antennas Propag. (EuCAP)*, Edinburgh, Scotland, Nov. 2007, p. 502.

[21] T. Fernandes, R. Caldeirinha, M. Al-Nuaimi, and J. Richter, "A discrete RET model for millimeter-wave propagation in isolated tree formations," *IEICE Trans. Commun.*, vols. E88–B, pp. 2411–2418, Jun. 2005.

[22] S. Morgadinho *et al.*, "Time-variant radio channel characterization and modelling of vegetation media at millimeter-wave frequency," *IEEE Trans. Antennas Propag.*, vol. 60, no. 3, pp. 1557–1568, Mar. 2012.

[23] F. Wang, "Physics-based modeling of wave propagation for terrestrial and space communications," Ph.D. dissertation, Dept. Elect. Eng., Univ. Michigan, Ann Arbor, MI, USA, 2006.

[24] Y. L. C. de Jong and M. H. A. J. Herben, "A tree-scattering model for improved propagation prediction in urban microcells," *IEEE Trans. Veh. Technol.*, vol. 53, no. 2, pp. 503–513, Mar. 2004.

[25] K. Chee, F. Catalán, S. Torrico, and T. Kürner, "Modeling tree scattering in rural residential areas at 3.5 GHz," *Radio Sci.*, vol. 49, pp. 44–52, Jan. 2014.

[26] N. Leonor, R. Caldeirinha, T. Fernandes, D. Ferreira, and M. G. Sánchez, "A 2D ray-tracing based model for micro-and millimeter-wave propagation through vegetation," *IEEE Trans. Antennas Propag.*, vol. 62, no. 12, pp. 6443–6453, Dec. 2014.

[27] N. Rogers *et al.*, "A generic model of 1-60 GHz radio propagation through vegetation—Final report," QinetiQ, Farnborough, U.K., Tech. Rep. QINETIQ/KI/COM/CR020196/1.0, May 2002.

[28] F. T. Ulaby, T. E. Van Deventer, J. R. East, T. F. Haddock, and M. E. Coluzzi, "Millimeter-wave bistatic scattering from ground and vegetation targets," *IEEE Trans. Geosci. Remote Sens.*, vol. GRS-26, no. 3, pp. 229–243, May 1988.

NUNO R. LEONOR (S'15–M'18) was born in Leiria, Portugal, in 1988. He received the Licenciatura and M.Sc. degrees in electrical and electronics engineering (telecommunications) from the School of Technology and Management, Polytechnic Institute of Leiria, Leiria, Portugal, in 2010 and 2012, respectively.

He received the Ph.D. degree in teoría de la información y las comunicaciones from the University of Vigo, Vigo, Spain, in 2018, for his research program—A generic doubly-selective 3-D vegetation model using point scatterers.

He is currently a Researcher with the Instituto de Telecomunicações, Leiria, Portugal, and a Lecturer with the School of Technology and Management, Polytechnic Institute of Leiria, Leiria.

MANUEL GARCÍA SÁNCHEZ (S'88–M'93) received the Ingeniero de Telecomunicación degree from the Universidad de Santiago de Compostela, Spain, in 1990, and the Doctor Ingeniero de Telecomunicación (Ph.D.) degree from the Universidad de Vigo, Spain, in 1996.

His research interests include the studies of indoor and outdoor radio channel sounding and modeling for narrow- and wide-band applications at microwave and millimeter wave frequencies, point-to-multipoint radio links, mobile communications, UMTS, WLANs, and DVB-T distribution networks.

TELMO R. FERNANDES (S'05–M'06) received the Licenciatura degree in electrical engineering, telecommunications and electronics and the M.Sc. degree from the Faculty of Sciences and Technology of the University of Coimbra, Portugal, in 1996 and 2000, respectively, for his study—Channel Assignment on Cellular Networks using Neural Networks and Genetic Algorithms.

He received the Ph.D. degree in radiocommunication systems from the University of Glamorgan, Glamorgan, U.K., in 2007, for his research Program in radiowave propagation through vegetation. In 1997, he joined the School of Technology and Management, Polytechnic Institute of Leiria, Leiria, where he is currently a Senior Lecturer. He is currently a Researcher with the Instituto de Telecomunicações, Leiria, Portugal.

RAFAEL F. S. CALDEIRINHA (M'00–SM'15) was born in Leiria, Portugal, in 1974. He received the B.Eng. degree (Hons.) in electronic and communication engineering and the Ph.D. degree in radiowave propagation, for his research work in vegetation studies at frequencies from 1 to 62.4 GHz, from the University of Glamorgan, U.K., in 1997, and 2001, respectively. He is currently the Head of the Antennas and Propagation Research Group, Instituto de Telecomunicações, Leiria, Portugal, and a Coordinator Professor in mobile communications with the School of Technology and Management, Polytechnic Institute of Leiria, Portugal.

His research interests include the studies of radiowave propagation through vegetation media, radio channel sounding, and modeling and frequency selective surfaces for applications at microwave and millimeter wave frequencies.

He has authored or co-authored over 90 papers in conferences and international journals, one book chapter and four contributions to ITU-R Study Group which formed the basis of the ITU-R P.833-5 (2005) recommendation. He was a fellow of IET. He was the Program Chair of the WINSYS International Conference from 2006 to 2012 and an Appointed Officer for the Awards and Recognitions of the IEEE Portugal section in 2014.